Adequacy Studies of Different Renewable Resources Using Monte Carlo Simulation Method

Amir Ghaedi [1]*, Reza Sedaghati [2], Mehrdad Mahmoudian [3]

[1]Department of Electrical Engineering, Dariun Branch, Islamic Azad University, Dariun, Iran, amir.ghaedi@miau.ac.ir
[2]Department of Electrical Engineering, Beyza Branch, Islamic Azad University, Beyza, Iran, reza.sedaghati@iau.ac.ir
[3]Department of Electrical and Electronic Engineering, Shiraz University of Technology, Shiraz, Iran, m.mahmoudian@sutech.ac.ir

Abstract

Produced power of wind, solar, run of the river, ocean thermal, tidal and wave power plants is respectively, dependent on wind velocity, sun radiation, river flow, temperature of ocean upstream, period & height of waves, tidal level or tidal stream velocity. Due to wide change in these quantities, produced power of these renewable resources changes a lot over time. As the penetration level of renewable resources in electric network is increased, reliability and other aspects of electric network may be affected that should be studied. Analytical method is not suitable to study uncertainties of output power of renewable resources in reliability analysis of electric network with these renewable power plants. Thus, the current research suggests Monte Carlo simulation method to study effect of renewable power plants on reliability indices. Renewable power plants studied in the research are wind turbines, solar farms, wave energy converters, run of the river power plants, both types of tidal units, and ocean thermal energy conversion systems. Numerical studies are performed on test electric networks, to study these renewable resources impact on reliability indices of electric networks with renewable power plants. It is concluded from numerical outcomes that these renewable power plants improve reliability performance of electric network. However, due to the variation of renewable resources, the impact of renewable power plants on reliability performance of the electric network is less than the conventional units with the same capacity.

Keywords: reliability, renewable resources, Monte Carlo simulation, power plants.
Article history: Received 2023/10/27; Revised 2023/12/15; Accepted 2024/01/10, Article Type: Research paper

https://doi.org/10.30495/ijsee. 2024.1999935.1292

1. Introduction

The greenhouse gases including CO_2, SO_2 and NO_X are produced from fossil fuels burning that results in the environmental problems. Due to these environmental effects of fossil fuel-based power plants and the sudden increase in the oil prices in 1970s, electric companies have decided use renewable power plants. Thus, renewable power plants including wind, solar, run-of-the-river, wave, tidal and ocean thermal energy conversion systems are constructed in electric networks. The output power of wind turbines, photovoltaic farms, wave energy converters, ocean thermal energy conversion systems, run of the river plants, current kind and barrage kind tidal units is proportional to wind velocity, sun radiation, height & period of waves, temperature of ocean upstream, water flow rate, tidal current speeds and tidal height. Wide change in renewable quantities makes produced power of renewable resources changes a lot. Despite the numerous benefits of the renewable power plants, change in output power of them over time makes different aspects such as reliability of electric networks with large-scale renewable resources are affected. Thus, development of new methods is required to study effects of renewable power plants on electric networks. In this regard, many researchers studied reliability analysis of electric network with renewable power plants. In [1], reliability of electric network with large capacity wind units is evaluated by analytical approach. In this paper, in the proposed multi-state reliability presentation of wind turbines equipped to double fed induction generator, components failure and variable output are addressed. According to this presentation, adequacy studies of electric network with wind farms are performed. In [2], large-scale

photovoltaic units are presented with multi-state model. The suggested model is utilized in analytical reliability analysis of electric network incorporating PV farms. The research concludes it can be neglected from components failure in reliability presentation of PV unit. Thus, multi-state reliability presentation of PV units can model change in output power that is proportional to sun radiation. In [3], a run of the river power plant composed of fore bay tank, filter, penstock, main valves, generators, transformers and turbines are studied. In this research, components failure and change in output that is proportional to water flow rate are addressed in the reliability presentation of plant. The suggested reliability presentation is utilized for reliability analysis of electric network with ROR units. In [4], the effect of energy storage system on reliability indices of electric network with wind and solar energies is analysed. In this research, vanadium redox (VR) batteries with large capacity improves reliability of electric network incorporating PV and wind units. In [5] and [6], according to analytical method, adequacy analysis of electric network with tidal units is done. In [5], tidal barrage and in [6] tidal stream turbines as two kinds of tidal power plants are studied. In the suggested reliability presentations of these ocean power plants, components failure and change in tides are addressed. In [7], ocean thermal power plants are integrated in operation analysis of electric network by PJM technique. In the research, impact of closed-cycle OTEC systems on operation indices that results in improvement in electric network incorporating these ocean power plants, is analysed.

In [1-7], analytical techniques have been used for reliability evaluation of renewable resources including wind turbine, photovoltaic farm, run of the river power plant, barrage kind tidal power plant, stream kind tidal power plant and ocean thermal energy conversion systems. Uncertainties of renewable resources leads to change of output electric power produced by them. Thus, Monte Carlo simulation techniques, that can analyse reliability of electric network with renewable resources, is suggested, in this research, because, in variable environment, Monte Carlo method is better than analytical approaches. It is due to the compatibility of simulation-based methods to variation of generated power over time. Thus, in the current research, Monte Carlo simulation technique is proposed to study effect of different renewable resources including wind turbines, PV farms, wave energy converters, barrage kind and stream kind tidal units, ocean thermal power plants and run of the river units on electric network reliability. To achieve this goal, this research is composed of follow sections. Second part includes introduction of different renewable resources including wind turbines, PV farms, ROR units, wave energy converters, OTEC systems, barrage kind and stream kind power plants. Reliability of electric network and suggested method, i.e. Monte Carlo approach used for reliability analysis of renewable-based power system, are introduced in the third section. Simulation of test networks for addressing effects of renewable resources, are interpreted in fourth part. Conclusions of research is summarized in fifth part.

2. Different Renewable Resources

In this section, renewable resources including wind turbines, photovoltaic farms, wave energy converters, run-of-the-river power plants, ocean thermal energy conversion systems and different types of tidal units, i.e. stream kind and barrage kind tidal units are described. Besides, composed components, electric energy production and associated power formula of these plants are discussed.

A) Wind Turbines

In wind turbines, conversion of air mass kinetic energy to the electricity is done. The generated power associated to an air mass with the speed of *v*, can be calculated as [8]:

$$P = \frac{1}{2} C_p \rho A v^3 \quad (1)$$

Where, ρ, A and C_P are density of air, turbine area and Betz coefficient. There are different technologies associated to electric generators connected to wind turbines. They are permanent magnet synchronous technology, double fed induction kind, synchronous type with electric exciter winding, double fed induction kind without brush, squirrel cage induction kind and wound rotor induction technology [8]. Typical structure for wind units with doubly fed induction electric generator (DFIG) is presented in Fig. 1. As can be seen, a DFIG-based wind plant is composed of wind turbines consist of tower and blades, gearbox, brake, mechanical control system and associated sensors, DFIG generator, electrical control system to control the electrical quantities of the plant and transformer. In DFIG technology an induction generator with wound rotor connected to rectifier-capacitor-inverter is used. The dependency between generated power of wind turbine on wind velocity is presented by power curve of turbines that is determined by the manufacturers. In Fig. 2, a typical power curve of wind turbines is presented. The figure presents generated power of wind turbines for speeds less than cut-in velocity and more than cut-out or cut-off wind velocity would be zero. The generated power of wind turbine for velocities more than cut-in

velocity and less than rated velocity is proportional to v^3 and output power in region more than v_{rated} and less than $v_{cut\text{-}off}$ would be constant, and is equal to rated power.

B) Photovoltaic(PV) Farms

Fig. 3 presents structure and facilities of typical photovoltaic farms including photovoltaic panels, DC-DC electric converters to track maximum power point and the inverters for converting DC generated power to AC power. As can be seen in the figure, a sub-array consists of several PV panels connected to a DC/DC converter, an array consists of several sub-arrays connected to an inverter and a PV farms consists of several arrays. A solar cell is a p-n junction that converts the solar radiation to the DC power. A PV panel is composed of several series and parallel solar cells to achieve higher voltage and current. The generated power of a PV farm is calculated by multiplying the solar radiation by the total area of PV panels and the efficiency of the farm including the efficiencies of electrical converters, PV panels, wires and connections [9].

C) Wave Energy Converters

The potential of wave energy around the world is estimated to be 2TW [10] and so, this kind of renewable resource is expected to have a significant contribution in electricity production. There are three types of wave energy converters including terminators, linear absorbers and point absorbers. The point absorbers are floating wave converters that their size is small compared to the swell wavelength. These converters can follow the wave movement and extract the energy of waves from any direction such as pressure activated point absorbers and heaving buoy point absorbers. The linear absorbers, such as pelamis, unlike point absorbers, must be moored so that their principle axis is maintained perpendicular to the oncoming waves. The terminators, such as oscillating water column and overtopping converters are other kind of wave generators. The power delivered by each meter of a wave can be calculated as[10]:

$$P = \frac{\rho g^2 H^2 T}{32\pi} \qquad (2)$$

Where, ρ is density of seawater and is considered to be 1025 kg/m^3, g is acceleration due to gravity that is 9.81 m/s^2, H is wave height and T is wave period. Produced power of wave generators depends on period and height of waves. Power matrix is defined for each wave generator to describe produced power versus height and period of waves that is determined by manufacturer of wave converter. In this paper, a wave generator with AquaBuoy technology is considered for studying reliability of this wave generator. Structure of this wave generator is presented in Fig. 4. This wave energy converter is a device that captures the energy from the vertical motion of the waves. The resulted up and down motion of the device, the floating tube connected to the converter responses and the piston attached to the end of this tube leads to the motion of hose pump. When the hose pump moves the water is pushed and drives impulse turbines connected to the generators and the electricity can be generated.

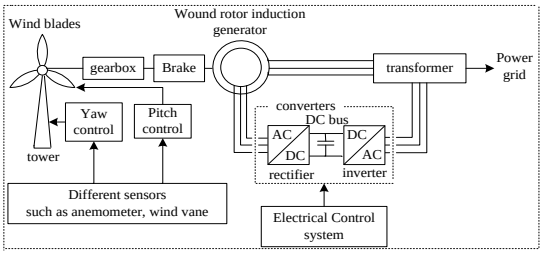

Fig. 1. Structure of wind turbines

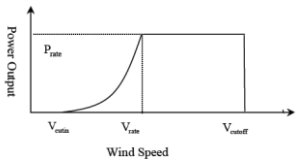

Fig. 2. Power curve for typical wind turbines

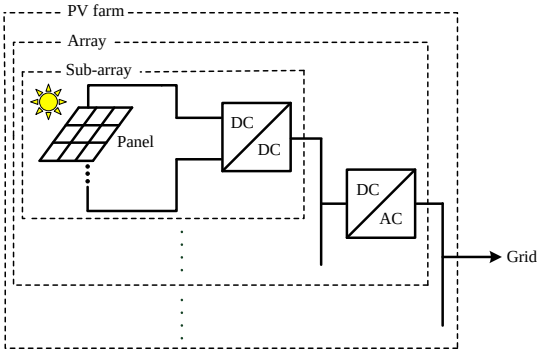

Fig. 3. The structure of typical PV farms

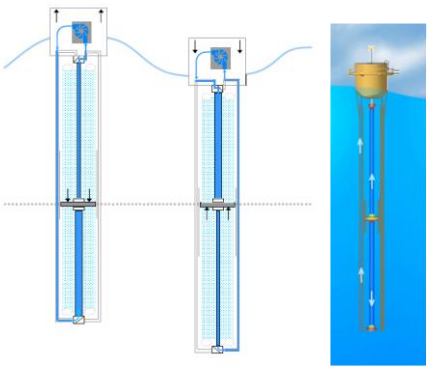

Fig. 4. The structure of AquaBuoy

D) Ocean Thermal Power Plants(OTEC)

The OTEC systems use difference between the temperature of waters in the ocean surface with 20-30^{0}C and the temperature of waters at 800-1000m deep with 4-5^{0}C to drive a thermodynamic Rankin cycle and generate the electricity. There are three types of OTEC systems including open-cycle, closed-cycle and hybrid power plants. In open-cycle power plant, seawater is used as working fluid. Ocean upstream water is pumped into a 0.03 bar flash evaporator. The low pressure of the evaporator leads the water to boil at 22^{0}C and the steam is generated. After it, produced steam turns the turbine. Electric generator connected to turbine, turns, too and produces electric energy. Steam coming out turbine enters into the condenser containing downstream water placed in depth of 800-1000m. Thus, the steam is converted to desalinized water. In closed-cycle OTEC units, low-boiling-point working fluid such as ammonia enters into evaporator containing warm water pumped from ocean upstream. Then, working fluid is vaporized and expands through a turbine connected to the generator to generate electricity. Then, the steam enters into the condenser containing the cold water is pumped from the depth of 800-1000m and is converted to the liquid. The hybrid OTEC system is a combination of open and closed-cycle OTEC units. In the current research, a closed-cycle OTEC power plant is integrated into test network for evaluating effect of OTEC power plants on reliability of electric network. Fig. 5 presents structure of a typical closed-cycle OTEC system [11].

The temperature versus entropy (T-S) associated to the thermodynamic Rankin cycle is presented in Fig. 5. Power produced by closed-cycle OTEC unit is described as [11].

E) Run of the River Power Plants

Fig. 7 presents structure of typical ROR plants and the composed components of them. A ROR plant consists of water channel, fare bay tank, filters, shoot, penstocks, main valves, turbines, generators and transformers. The water of a fast-moving river usually placed in the mountainous areas is conducted to the fore bay tank using of water channels.

Fore bay tank water transfers to turbines through the penstocks to generate the electricity using of the generators connected to the turbines. The turbine inlet water flow can be controlled using of the main valves. To prevent the entry of unwanted objects to the penstocks and turbines, the filter should be placed at the entrance of the penstocks. The shoot is another water channel that the water can be transferred from fore bay tank to power plant downstream, in off state of plant or very high flow of water. Produced power of ROR unit transmits to grid using of the transformers. Produced electric power of ROR unit depends on water flow rate. Thus, based on water rate data, power plant dimensions and the characteristics of the generator and turbines such as their efficiency, the generated power can be determined [12].

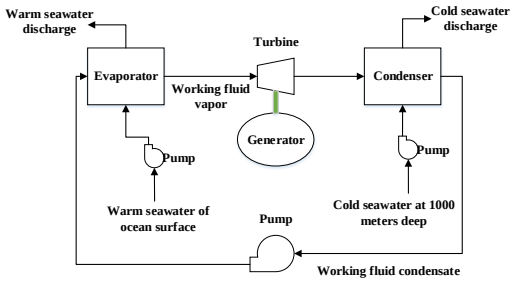

Fig. 5. Structure of closed-cycle OTEC system

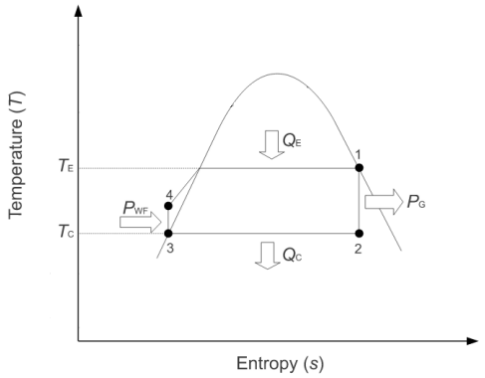

Fig. 6. T-S curve of Rankin cycle

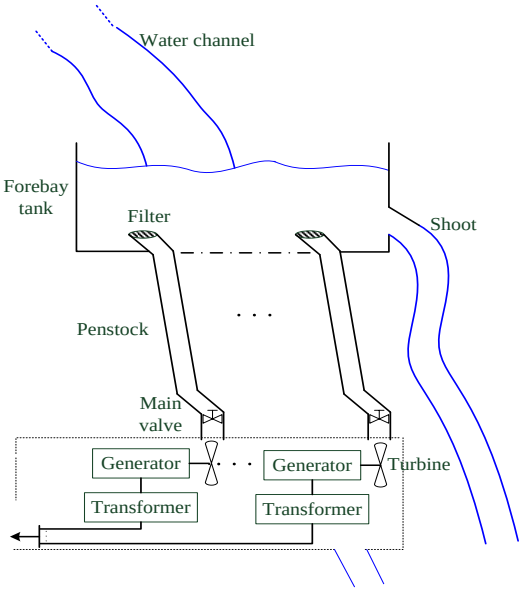

Fig. 7. The structure of the run-of-the-river power plant

F) Tidal Power Plants

The tides are occurred due to the relative motion of the earth and the moon relative to the sun. This phenomenon can appear as a change in the sea level or tidal current speed. There are two technologies to extract the energy of tides including barrage kind and stream kind tidal units. Fig. 8 shows structure of barrage kind tidal unit. In this plant, a dam is constructed between the sea and the reservoir. Occurrence of tides leads water transfers from sea to reservoir or in reverse direction. Turbines installed in sluices of the barrage are turned by water and electric energy is produced. There are three modes for electric power generation in barrage kind tidal units. They are production in ebb-state mode, production in flood-state mode and production at both ebb-flood-states mode. Table 1 presents the characteristics of three working modes of barrage kind tidal units.

The equations associated to electric power production by barrage kind tidal units operated in different modes are described in [13].

In second kind of tidal units, i.e. stream kind tidal power plants, tidal streams with specific velocity passing through stream-type turbines installed undersea produce electric power. Topology of stream kind tidal units and composed components including blades (current type tidal turbines), shaft and bearing, gearbox, different generators (such as permanent magnet synchronous technology, double fed induction kind, squirrel cage asynchronous type and synchronous technology with electric exciter winding), electrical converters, control system, cable and transformer are presented in Fig. 9 [14].

Produced electric power associated to a mass of moving water can be calculated as (1) similar to the generated power of a mass of air. However, in this case, ρ is density of seawater (1025 kg/m^3), A is area of the turbine and C_P is Betz coefficient. Dependency between produced electric power of stream kind tidal turbines on tidal stream velocity can be presented by the power curve developed by the manufacturer. Fig. 10 illustrates typical power curve of these stream turbines. In tidal stream turbines, electric power of tidal streams with velocities from zero to cut-in velocity would be zero. Produced electric power of turbine for the velocities from cut-in velocity to rated velocity is proportional to v^3 and generated power of turbine for velocities from rate velocity to rated velocity would be constant and is equal to rated electric power. Due to low value of tidal stream velocities, cut-out velocity for stream kind turbine is not occurred.

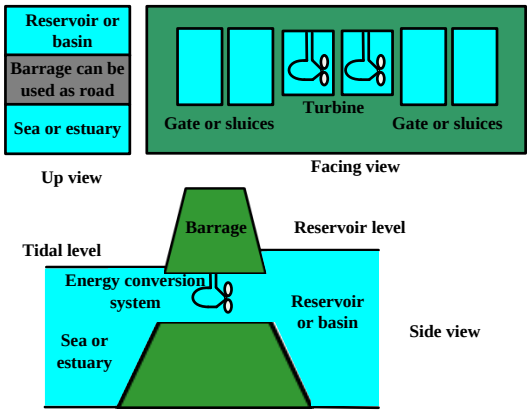

Fig. 8. The structure of the barrage type tidal power plant

Table.1.
Three working modes of barrage kind tidal units

Modes	Reservoir filling		Electric power production	
	State	Water transferring direction	State	Direction of water passing through turbines
Production in ebb-state mode	Flood	Sea - reservoir	Ebb	Reservoir - sea
Production in flood-state mode	Flood	Sea - reservoir	Flood	Sea - reservoir
Production in both ebb-flood-states mode	Flood	Sea - reservoir	Flood-ebb	Sea – reservoir and reservoir - sea

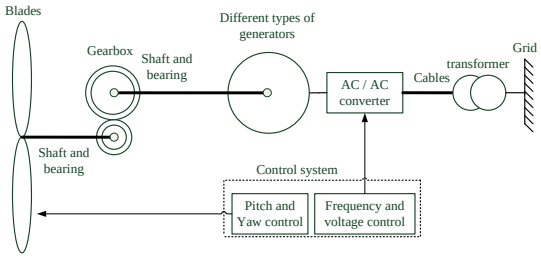

Fig. 9. The structure of stream kind tidal unit

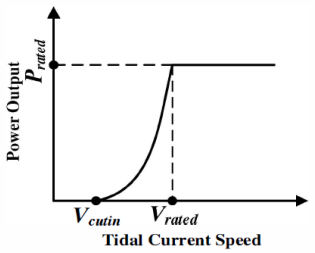

Fig. 10. The power curve of stream kind turbines

3. Monte Carlo Approach for Reliability Analysis of Renewable Resources

The power system consists of three subsystems including generation, transmission and distribution subsystems. Thus, three hierarchical levels (HL) are defined in reliability analysis of electric networks including HLI, HLII and HLIII [15]. In the reliability studies of HLI, HLII and HLIII, respectively the generation system, generation-transmission networks and entire power system containing three subsystems are evaluated. To analyse the reliability of the power system, two approaches including analytical and numerical methods are employed. In analytical method, all elements of power systems are modelled and using of the mathematical equations, different indices of electric networks are obtained. In numerical methods that usually use Monte Carlo technique, reliability indices are determined using of the simulation of the behaviour of the different element of the power system. Wide variation of produced electric power of renewable power plants leads number of states in model of renewable power plants is numerous. A model with numerous state cannot be used in analytical analysis of electric network reliability. However, due to the compatibility of Monte Carlo method to variation of produced electric power renewable power plants, this research suggests Monte Carlo method for adequacy assessment of electric network in HLI incorporating renewable power plants. In this study, the generation units and all demands are placed on common-bus, and transmission and distribution networks are neglected. Fig. 11 illustrates different steps of suggested method. In this method, the software produces random numbers at [0,1] for all equipment, or conventional generation units. The conventional generation units or elements can be modelled with two states including up or down. Availability (A) is probability of up state, and unavailability (U) is probability of down state of the unit or element. If produced random number is less than availability, associated unit or element would be in the up state, and if produced random number is more than availability, associated element or unit would be in the down state. In this study the Monte Carlo simulation is run for 1000 repetitions and average time of load interruption expressed by hours/year and average interrupted energy expressed by MWh/year are calculated.

4. Simulation of Test Networks

Here, using Monte Carlo simulation technique, numerical results associated to adequacy analysis of renewable-based electric network is conducted to analyse effect of wind turbines, PV farms, wave energy converters, barrage kind and stream kind tidal units, ROR power plants and OTEC systems on reliability indices of electric network is investigated. Hourly demand of electric network over a year based on IEEE standard load pattern is used [16] that is presented in per-unit scale in Fig. 12. The characteristic of test generation units i.e. Roy Billinton test network and IEEE test network are given in [17] and [18], respectively.

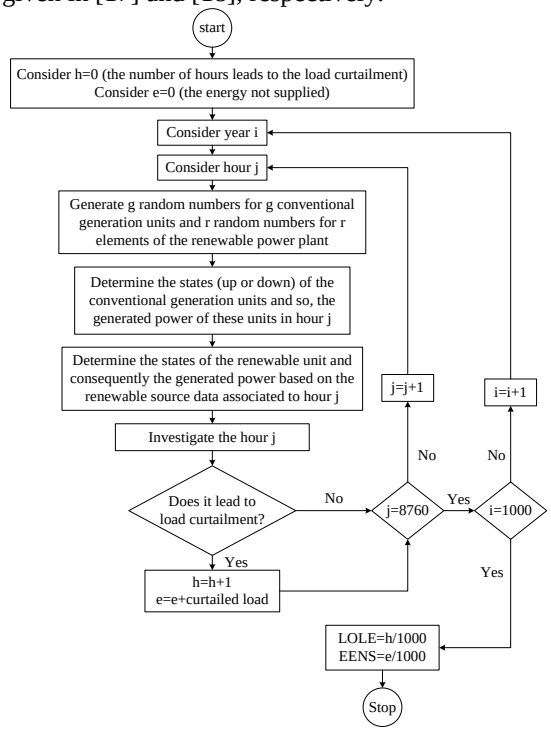

Fig. 11. The flowchart of the Monte Carlo technique

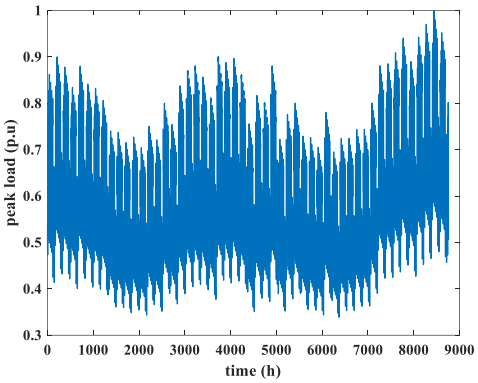

Fig. 12. The hourly peak load

A) Wind Turbines

The data associated to hourly wind velocity are presented in Fig. 13. In the current research, V164 technology with 8MW installed capacity is utilized as understudied wind turbine. The power curve V164 is presented in Fig. 14. Thus, hourly produced electric power of each V164 turbine is calculated and presented in Fig. 15. V164 component failure

and repair rates are collected by manufacturer or the operator of these wind turbines. In this paper, 5 failures per year and 100 hours are reliability parameters of understudied V164 turbine.

Here, reliability analysis Roy Billinton electric network when no unit is added to the network (case I), when 40 MW non-renewable power plant is added to the network (case II), and when wind farm consists of five 8MW wind turbine is added to the network (case II) is done. For non-renewable unit, 5 failure per year and 100h average repair time are considered.

The average time of interruption and average interrupted energy associated to the cases, when peak of demand is varied, are calculated using of the proposed technique and presented in Fig 16 and 17. The figures illustrate that reliability improves when wind units are added to test network. Nevertheless, impact of wind farm on reliability improvement is less than non-renewable power plants. Because of change in wind velocity, output electric power of wind farm changes, too. Thus, electric power of wind units is less than nominal value at more times of operation. Peak demand capability of network is maximum peak demand that network can provide while reliability index is satisfied. In this stage, peak demand capability of three cases with permissible average interrupted energy index are calculated provided that reliability index is less than 50MWh/yr. The values obtained for peak demand capability of case I, II and III are respectively, 204, 236 and 215MW. Thus, increase in peak demand capability of cases II and III would be 32 and 11MW, respectively.

B) PV Farms

A 30MW PV farm consists of 50 arrays each with 600kw capacity. Each array consists of 50 sub-arrays each with 12kw capacity. The sub-arrays are composed of 40 panels each with 300w capacity. The panel consists of 3 parallel branched that each branch is composed of 32 series solar cells. The capacity of DC/DC converters and inverters are respectively would be 12kw and 600kw. The panel efficiency is considered to be %18.4 and the efficiency associated to the other elements is assumed to be %90. The generated power of each panel in the 900w sun radiation is 300w/m^2 and so, electric produced power of farm would be 30MW at 900 w/m^2 solar radiation. Failure rate and average repair time of arrays are considered to be 1 failure during year and 100 hours, respectively.

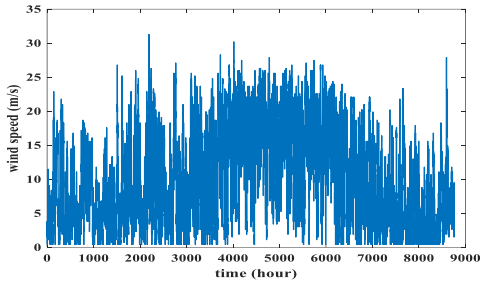

Fig. 13. The hourly wind speed

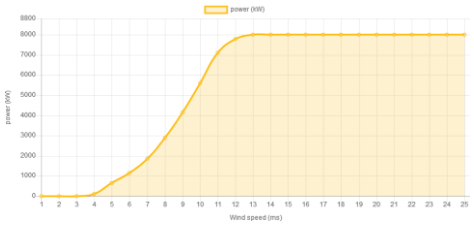
Fig. 14. The power curve of wind turbine based on the V164

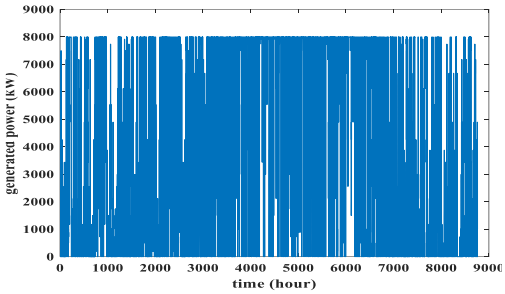

Fig. 15. The generated power of understudied wind turbine

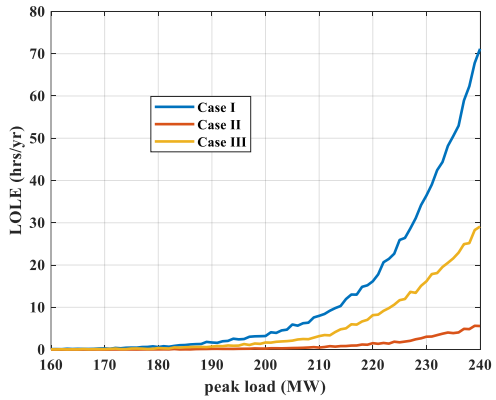

Fig. 16. The average time of interruption versus demand

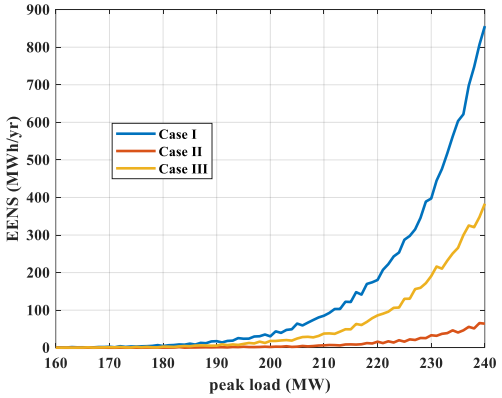

Fig. 17. The average interrupted energy versus demand

Hourly solar radiation is presented in Fig. 18. Here, adequacy analysis of Roy Billinton test network as case I, the network with non-renewable 30MW power plant as case II, and the network with understudied 30MW PV farm as case III, is dine. Five failure during year and 100 hours are considered for non-renewable power plant. For three cases, the average time of interruption and average interrupted energy at different demands are obtained using of the proposed technique and presented in Fig 19 and 20. The figures presents that addition of PV farm to the network makes improvement of adequacy indices. Nevertheless, because of change in electric power of PV unit arisen from change in sun radiation, reliability enhancement of non-renewable units is more than PV farm. The peak demand capability of the cases is calculated when average interrupted energy is less than 100MWh/yr. The obtained values for PLCC of cases I, II and III are, respectively, 212, 239 and 218MW, and so, increase in peak demand capability of cases II and III would be 27 and 6MW respectively.

C) Wave Energy Converters

Here, 30MW wave energy farm is studied that consists of 120 wave generators 250kw with AquaBuoy technology. Average repair and failure rate of each buoy are 98 and 2 times during year, respectively. Power matrix of AquaBuoy is presented in table 2. Hourly height and period of waves are presented in Fig. 21 and 22, respectively. Electric produced power of each buoy is determined by power matrix and hourly wave data. Fig. 23 presents hourly electric power of wave generator. Here, Roy Billinton test network and wave energy farm added to the test network are considered as cases I and II, respectively.

Average time of interruption and average interrupted energy related to cases I and II, at different demands are determined and illustrated in tables 3 and 4, respectively. Then, reliability evaluation of IEEE test network is performed. For this purpose, IEEE test network as case I, and the wave energy farm added to the test network as case II are analysed. Average time of interruption and average interrupted energy at different demands for the cases are determined and illustrated in tables 4 and 5, respectively. These tables present wave energy farms improve adequacy indices of both test networks. However, wide variation in wave quantities makes electric produced power of wave energy farms changes over time. Thus, electric produced power of wave energy farm is less than rated value in most of time. Therefore, the improvement in the reliability indices arisen from integration the wave converters is less than non-renewable power plants.

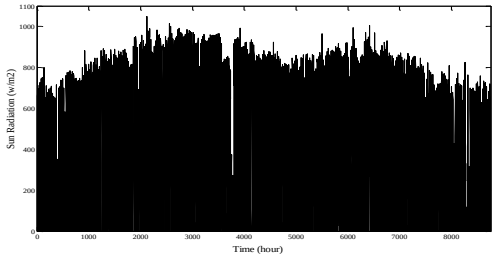

Fig. 18. The hourly solar radiation data

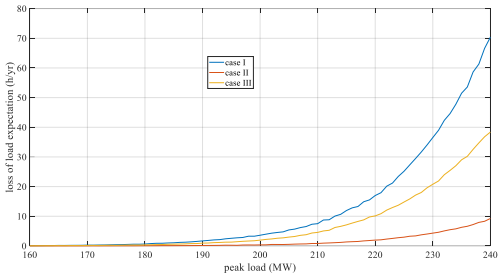

Fig. 19. The average time of interruption versus demand

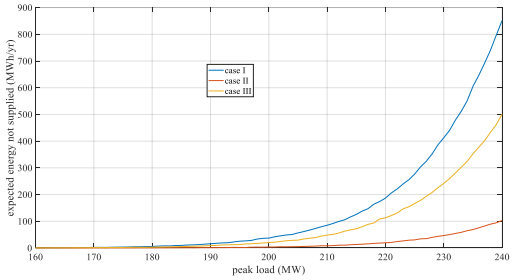

Fig. 20. The average interrupted energy versus demand

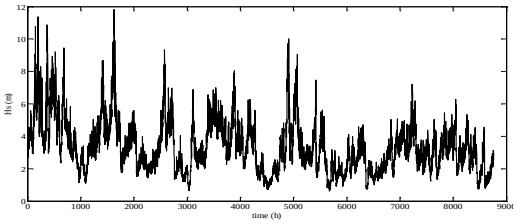

Fig. 21. Wave height

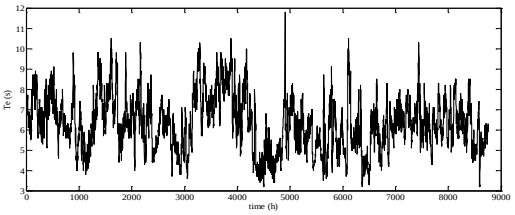

Fig. 22. Wave period

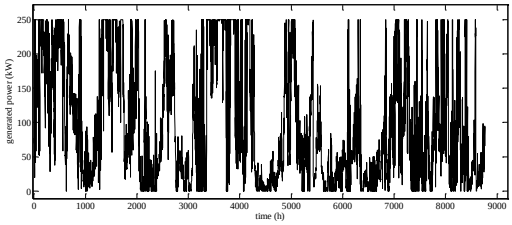

Fig. 23. Produced power of each buoy

Table.2.
AquaBuoy power matrix

Tp(s).Hs(m)	Power matrix (in Kw)												
	5	6	7	8	9	10	11	12	13	14	15	16	17
1	0	0	8	11	12	11	10	8	7	0	0	0	0
1.5	0	13	17	25	27	26	23	19	15	12	12	12	7
2	0	24	30	44	49	47	41	34	28	23	23	23	12
2.5	0	37	47	69	77	73	64	54	43	36	36	36	19
3	0	54	68	99	111	106	92	77	63	51	51	51	27
3.5	0	0	93	135	152	144	126	105	86	70	70	70	38
4	0	0	0	122	176	198	188	164	137	112	91	91	49
4.5	0	0	0	223	250	239	208	173	142	115	115	115	62
5	0	0	0	250	250	250	250	214	175	142	142	142	77
5.5	0	0	0	250	250	250	250	250	211	172	172	172	92

Table.3.
Average time of interruption versus demand of Roy Billinton

Case II	*Case I*	*Peak load (MW)*
0.09	0.29	170
0.28	0.41	175
0.38	0.59	180
0.5	0.99	185
0.87	1.69	190
1.26	2.66	195
1.34	3.55	200
2.93	5.53	205
3.68	7.71	210
6.42	11.67	215
9.36	17.09	220
13.65	26.64	225
19.07	37.2	230

Table.4.
Average interrupted energy versus demand of Roy Billinton

Case II	*Case I*	*Peak load (MW)*
0.7738	1.9739	170
2.0665	3.2173	175
2.9241	4.6022	180
5.87	8.5620	185
7.2973	15.8581	190
11.0715	27.4491	195
13.5653	36.7078	200
30.4473	57.9073	205
35.2391	87.4164	210
62.6093	126.3092	215
101.4234	188.8776	220
150.9344	298.8495	225
220.1766	420.5704	230

Table.5.
Average time of interruption versus demand of IEEE

Case II	*Case I*	*Peak load (MW)*
5.82	6.6	2800
8.48	9.48	2850
11.57	12.73	2900
15.67	16.96	2950
21.41	22.24	3000
29	30.67	3050
38.18	40.12	3100
47.87	53.28	3150
63.78	68	3200
81.52	88.62	3250
102.84	108.99	3300
129.78	136.32	3350
159.64	169.73	3400

Table.6.
Average interrupted energy versus demand of IEEE test network

Case II	*Case I*	*Peak load (MW)*
751.3869	801.2028	2800
1002.3	1106	2850
1522	1676.2	2900
2029	2218	2950
2931.2	3019.4	3000
4034.2	4221.6	3050
5596.2	5873.9	3100
7179.1	8045.6	3150
9621.9	10662	3200
12963	14091	3250
16887	18039	3300
22046	23204	3350
27927	29948	3400

D) Ocean Thermal Energy Conversion Systems

In this part, an OTEC unit with 30 MW installed capacity utilized ammonia as working fluid is considered. The ocean upstream temperature at each hour is presented in Fig. 24. The temperature of the cold water at the depth of 800-1000m is considered to be 4^0C. The thermodynamic characteristic of ammonia for temperatures between 20 to 26^0C is required to determine the electric power produced by OTEC unit [7]. Based on the thermodynamic equations, we calculate produced electric power of understudied OTEC unit at each hour and present the results in Fig. 25. Reliability data including both average failure rate and average repair time of composed components of OTEC system is required to determine the reliability indices of electric network integrated with OTEC unit [7]. According to proposed technique, we calculate average time of interruption and average interrupted energy considering peak load for RBTS and RBTS integrated to the understudied OTEC system as cases I and II, and illustrate the results in Figs. 26 and 27.

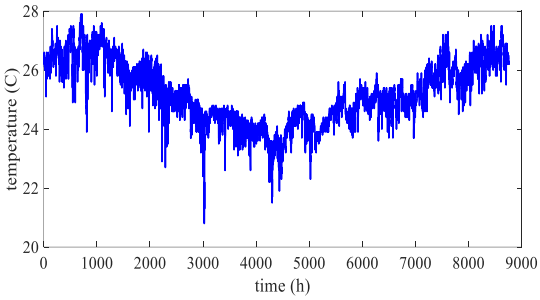

Fig. 24. Hourly temperature of ocean surface

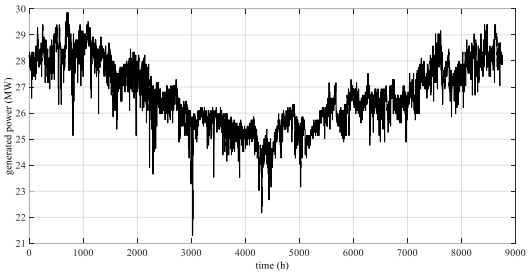

Fig. 25. The hourly generated power of OTEC plant

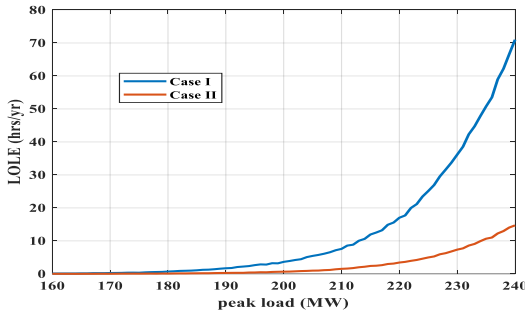

Fig. 26. The average time of interruption at different demands

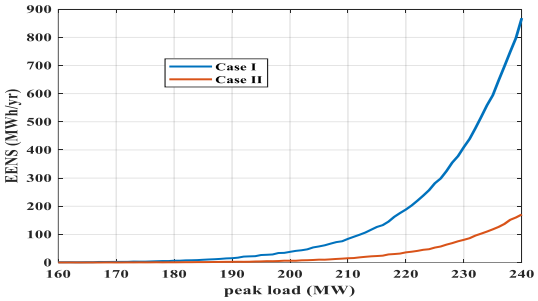

Fig. 27. The average interrupted energy at different demands

Here, we evaluate adequacy of IEEE-RTS considering effect of OTEC unit. We study IEEE test network and IEEE network containing OTEC unit as cases I and II. We calculate average time of interruption and average interrupted energy related to these two cases considering different peak loads, and present the results Figs. 28 and 29, respectively. We conclude that addition of ocean thermal energy conversion system to RBTS and IEEE-RTS, improves reliability indices of these two systems. However, temperature of ocean upstream changes that leads produced electric power of OTEC unit varies over time. Thus, produced electric power of OTEC system is less than the rated capacity in the most of time. For this reason, reliability enhancement of OTEC unit is less than the same-sized conventional units.

E) Run of the River Units

Here, a 30MW ROR farm consists of 5 ROR-plants that each plant is composed of 4 penstocks. Each penstock can conduct the water to a 1.5MW turbine and generate the electricity. The rated power can be generated when the water flow is equal to the nominal water flow (2.2 m^3/s). The hourly water flow is presented in Fig. 30. We present reliability data of composed elements of ROR plant in table 8.

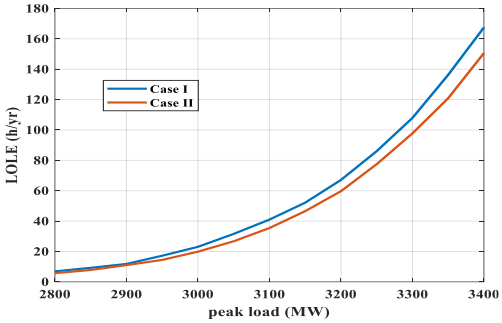

Fig. 28. The average time of interruption at different demands

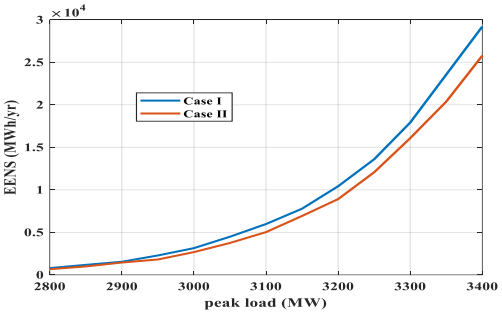

Fig. 29. The average interrupted energy at different demands

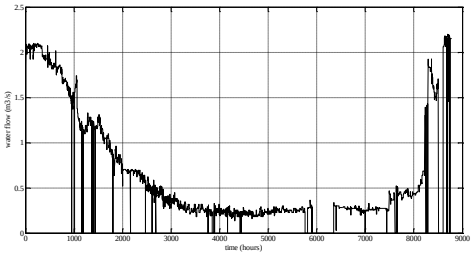

Fig. 30. The hourly water flow

Table.7.
The reliability parameters of the composed components of ROR plant

Components	*Failure rate (number per year)*	*Average time of repair (hour)*
Water channel	zero	-
Fore bay	zero	-
Filter	2	10
Penstock	zero	-
Main valve	0.5	87.6
Turbine	0.5	87.6
Generator	0.2	175.2
Transformer	0.2	175.2
Shoot	zero	-

For evaluating impact of ROR plant on RBTS reliability, we consider three cases including: case I is RBTS, case II is the RBTS integrated to the understudied ROR plant and case III is RBTS containing a 30MW traditional unit specified by unavailability of 0.05. we calculate average time of interruption and average interrupted energy of these cases and presente in tables 8 and 9. We conclude ROR plant enhances reliability of electric networks. However, uncertainty of these renewable resources leads improvement in reliability indices of ROR plant case is less than the conventional unit case. In table 9, we also present equivalent conventional capacities associated to ROR plant at different demands. As can be seen from the results that change of output power of ROR plant makes effect of 30MW ROR unit in the reliability improvement is equal to the effect of a traditional unit with capacity around 6-7MW.

For evaluating impact of ROR units on IEEE test network reliability, one to five conventional and ROR units are added to this system. We calculate average time of interruption, average interrupted energy and permissible increased demand of related cases in 2850MW peak load, and illustrate the results in table 10. We conclude ROR plants improve reliability of power network. However, effect of ROR units on reliability improvement of electric network is less than conventional ones.

F) Tidal Power Plants

In this part, a 30MW barrage kind tidal unit consists 12 Kaplan turbine with 2.5MW capacity is considered to study the effect of barrage kind tidal unit on RBTS reliability. The hourly level of tides can be presented by (3):

$$l(t) = l_0 + \sum_{k=1}^{n} l_k \cos(u_k t + x_k) \quad (3)$$

Where, l(t) is level of tides at time t, u_k, l_k, x_k are angular velocity, tidal level and phase of tides associated to k^{th} component, and l_0 is DC component of tidal level. Here, different harmonic components of the tides are presented in table 11, and so, variation of level of tides is presented in Fig. 31. Based on the bathymetry studies performed on the reservoir, basin volume can be obtained versus its level. In understudied barrage kind tidal unit, basin volume considering basin height are presented in Fig. 32. In this study, due to the reservoir constraints, the basin height is assumed to remain between 2.5 and 4.5m. The hydro-turbines of plant produces electricity at water head higher than 1m. besides, turbine efficiency is considered to be %90. The barrage kind tidal unit operates in ebb generation mode. Based on related power equations of unit, the hourly generated power is calculated and presented in Fig. 33. In the bottom of the figure, to make the figure look better, part of it has been enlarged and presented. We present reliability data of composed elements in table 12.

Table.8.
Average time of interruption versus demand

Case III	*Case II*	*Case I*	*Peak load (MW)*
0.247445	1.832781	3.57143	170
0.428037	2.909058	4.967642	175
0.602653	4.05321	6.35791	180
0.963396	6.018318	11.12279	185
1.328097	9.408126	15.65325	190
2.781695	13.22548	20.74907	195
4.202168	17.56675	26.35622	200
7.463669	30.65807	68.68322	205
10.62894	58.71933	109.0098	210
16.50375	89.72251	148.1956	215
22.16009	122.0685	186.307	220
29.93379	162.898	256.9655	225
38.01036	219.0237	324.7104	230

Table.9.
Average interrupted energy versus demand

Eq. conv. Cap. (MW)	*Case III*	*Case II*	*Case I*	*Peak load (MW)*
5.85	2.175809	13.46854	28.52964	170
6.78	3.784765	24.76691	48.80883	175
6.78	6.22678	41.21717	75.42479	180
7.12	9.933107	64.15553	116.6625	185
6.73	15.33735	100.3598	179.8059	190
6.96	25.13382	153.5238	265.2044	195
7.15	41.79177	225.4976	375.0485	200
7.07	69.68175	330.7624	601.9086	205
6.16	112.8116	541.953	1027.752	210
6.43	177.4043	896.2195	1640.571	215
6.72	269.0979	1398.77	2431.18	220
7.25	392.1264	2063.892	3475.057	225
7.24	551.8419	2961.29	4839.823	230

Table.10.
Reliability indices

Added Units	*LOLE (h/yr)*	*EENS (MWh/yr)*	*IPLCC (MW)*
Base Case	112.9085	16983.86	0
Base case + 1 conv.	95.32231	14036.8	29.6
Base case + 2 conv.	80.73625	11549.94	59.5
Base case + 3 conv.	68.86317	9431.269	89.3
Base case + 4 conv.	58.22836	7630.917	119.0
Base case + 5 conv.	48.45224	6119.975	148.6
Base case + 1 ROR.	107.2386	16029.97	9.3
Base case + 2 ROR.	101.7935	15124.72	18.2
Base case + 3 ROR.	96.61983	14265.67	27.4
Base case + 4 ROR.	91.45622	13365.25	36.3
Base case + 5 ROR.	87.00219	12298.94	45.2

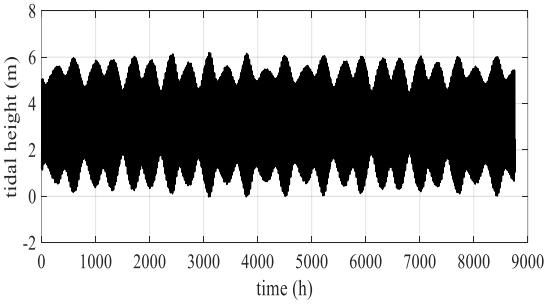

Fig. 31. The hourly tidal level

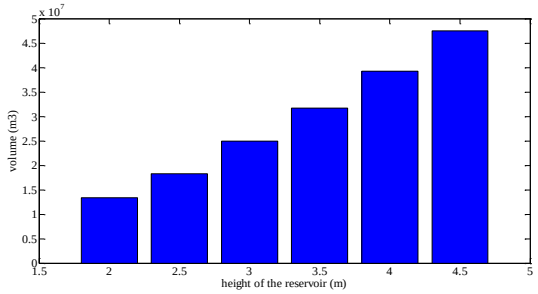

Fig. 32. The basin volume considering basin height

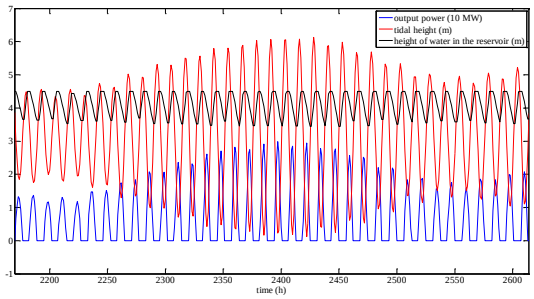

Fig. 33. Level of tides, basin height and produced power of tidal unit at each hour

Table.11.
The harmonic components of tidal level

components	Angular velocity (cycle per hour)	level (centimetre)	Phase (^{0})
l_0 (average tide)	0	317.0	0.00
M2	0.08051	210.140	157.6
S2	0.08333	57.932	264.4
N2	0.07900	38.079	80.2
K2	0.08356	16.952	69.0
L2	0.08202	13.849	35.6
K1	0.04178	10.237	71.1
NU2	0.07920	10.149	131.9
O1	0.03873	9.825	343.1
MU2	0.07769	9.342	181.9
2N2	0.07749	7.920	19.4
LDA2	0.08182	5.529	321.6
M4	0.16102	4.907	100.5
SSA	0.00023	4.079	249.1
MSN2	0.08485	3.233	115.7
M6	0.24153	3.188	161.1
EPS2	0.07618	3.121	76.0
2MS6	0.24436	3.101	258.3
P1	0.04155	3.042	73.3
MS4	0.16384	2.413	241.4
OQ2	0.07598	2.140	307.1
M3	0.12077	2.014	74.5
MF	0.00305	1.900	225.4
MKS2	0.08074	1.842	89.2
2MN6	0.24002	1.756	79.6
Q1	0.03722	1.687	264.6
MN4	0.15951	1.432	32.0
MO3	0.11924	1.344	52.5
NO1	0.04027	1.167	341.0
MM	0.00151	1.096	62.2
MSF	0.00282	1.049	305.6
2SM6	0.24718	1.029	356.8

Table.12.
Reliability data of composed elements of barrage kind tidal plant

Components	Failure rate (number per year)	Average time of repair (hour)
Sluice	5	50
Turbine	5	100
Generator	5	50
Cable	5	200
Transformer	5	200

In this study, three cases are considered for evaluating effect of barrage kind tidal units on RBTS reliability. Case I is RBTS and in cases II and III, respectively, a 30MW traditional unit (λ=5 number per year, and r=100 hours) and mentioned barrage kind tidal unit are incorporated to RBTS. We calculate average time of interruption and average interrupted energy of these three cases and illustrate in Figs. 34 and 35. We also calculate permissible demand of cases I, II and III that the obtained values of them are 212, 239 and 216MW, respectively. Thus, the permissible increased demand of cases II and III are, respectively 27 and 4MW.

In this part, for investigating effect of stream kind tidal unit on RBTS reliability, a 30MW stream kind tidal unit consists 15 stream turbines is considered. The turbines are based on the 2MW SeaGen technology that the power curve of them is presented in Fig. 36. The tidal stream velocity is presented in Fig. 37. Based on hourly tidal stream velocity and power curve of stream type turbine, we calculate hourly produced electric power of unit and present the results in Fig. 38. We consider rate of failure and rate of repair associated to stream kind tidal turbine 2 failures per year and 98 repairs per year. We calculate average time of interruption and average interrupted energy of RBTS as case I and RBTS integrated to stream kind tidal unit as case II and illustrate the results in table 13 and 14.

To study the effect of current type tidal power plant on reliability of IEEE test network, we consider two cases including: case I is IEEE test network and in case II, the stream kind tidal unit is incorporated to IEEE test network. We calculate average time of interruption and average interrupted energy of these cases and illustrate in tables 15 and 16. We conclude that stream kind and barrage kind tidal units enhance reliability of electric networks. Besides, the tides vary, and so, produced electric power of tidal power plants changes. Thus, the effect of these renewable generation units in the reliability improvement of the power network is less than traditional plants with equal capacities.

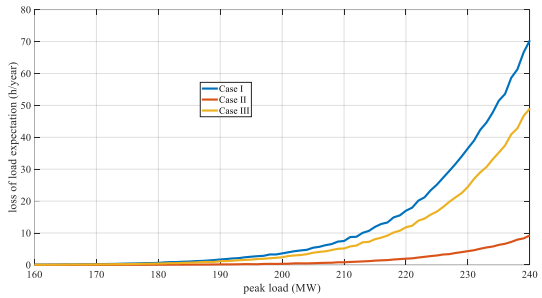

Fig. 34. The average time of interruption at different demand

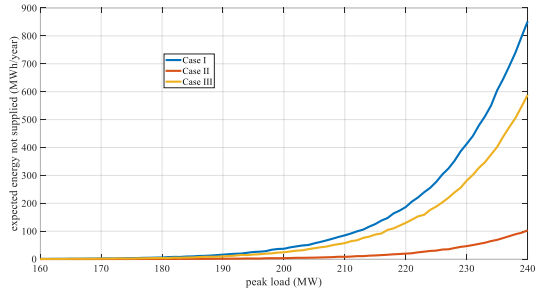

Fig. 35. The average interrupted energy at different demands

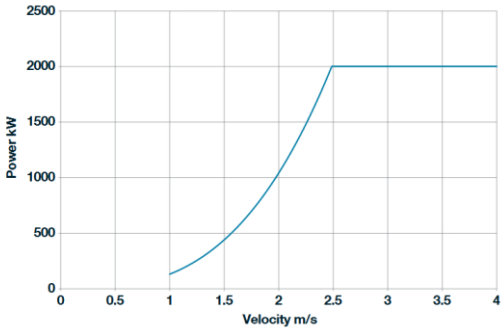

Fig. 36. Power curve of the current type turbines based on the SeaGen technology

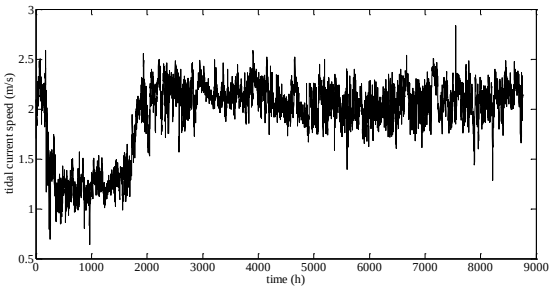

Fig. 37. The hourly tidal current speed

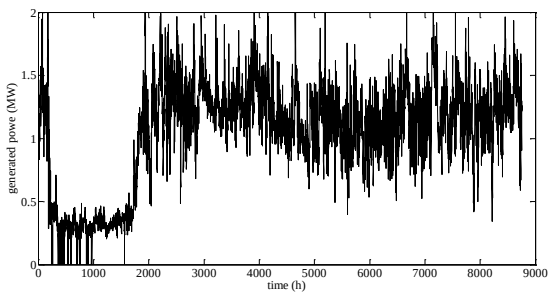

Fig. 38. The hourly produced electric power of stream kind tidal

Table.13.
Average time of interruption versus demand

Case II	***Case I***	***Peak load (MW)***
0.02	0.29	170
0.04	0.41	175
0.06	0.59	180
0.16	0.99	185
0.43	1.69	190
0.56	2.66	195
0.92	3.55	200
1.32	5.53	205
2.12	7.71	210
2.55	11.67	215
4.20	17.09	220
6.10	26.64	225
8.45	37.2	230

Table.14.
The average interrupted energy versus demand

Case II	Case I	Peak load (MW)
0.0620	1.9739	170
0.3052	3.2173	175
0.6238	4.6022	180
0.9275	8.5620	185
2.6222	15.8581	190
4.6154	27.4491	195
8.3663	36.7078	200
12.6157	57.9073	205
22.4270	87.4164	210
28.3299	126.3092	215
44.7569	188.8776	220
64.9081	298.8495	225
102.8604	420.5704	230

Table.15.
The average time of interruption versus demand

Case II	***Case I***	***Peak load (MW)***
5.87	6.6	2800
8.12	9.48	2850
11.97	12.73	2900
15.58	16.96	2950
21.2	22.24	3000
27.49	30.67	3050
36.18	40.12	3100
48.73	53.28	3150
61.15	68	3200
78.54	88.62	3250
99.27	108.99	3300
125.71	136.32	3350
154.22	169.73	3400

Table.16.
The average interrupted energy versus demand

Case II	***Case I***	***Peak load (MW)***
719.9549	801.2028	2800
986.8073	1106	2850
1528.3	1676.2	2900
2091.6	2218	2950
2799.1	3019.4	3000
3808.2	4221.6	3050
5303.6	5873.9	3100
7321	8045.6	3150
9230	10662	3200
12407	14091	3250
16162	18039	3300
21513	23204	3350
26709	29948	3400

5. Conclusion

In this paper, a numerical method based on Monte Carlo simulation approach is proposed for studying adequacy of renewable energy-based power systems. In this method, the condition of generation units and consequently total generated power associated to each hour is determined by generating random numbers. The amount of hourly curtailed load is determined by comparing generating capacity and related demand. By repetition Monte Carlo method, we calculate reliability indices. Adequacy assessment of electric network containing different renewable resources including wind turbines, photovoltaic farms, run of the river units, ocean thermal energy conversion systems, wave energy converters, barrage kind and stream kind tidal units are studied to address the variation of renewable resources including wind velocity, sun radiation, flow rate of water, temperature of ocean upstream, wave height and wave period, tidal current speed and tidal height. It is deduced from numerical outcomes of reliability analysis of RBTS and IEEE test networks, that addition of conventional and renewable power plants to electric network makes reliability indices of network improve. However, due to the variation in the renewable resources, produced power of these units is less than rated capacity in the most of operation time. Thus, the impact of renewable power plants on reliability enhancement of electric network is less than conventional units with the same capacity.

References

[1] Amir Ghaedi, Ali Abbaspour, Mahmud Fotuhi-Firuzabad, Moein Moeini-Aghtaie, “Toward a comprehensive model of large-scale DFIG-based wind farms in adequacy assessment of power systems”, IEEE Transactions on Sustainable Energy, vol. 5, no. 1, pp. 55-63, 2013. DOI: 10.1109/TSTE.2013.2272947.

[2] Amir Ghaedi, Ali Abbaspour, Mahmoud Fotuhi-Friuzabad, Masood Parvania, “Incorporating Large Photovoltaic Farms in Power Generation System Adequacy Assessment”, Scientia Iranica, vol. 21, no. 3, pp. 924-934, 2014.

[3] Esmail Khalilzadeh, Mahmud Fotuhi-Firuzabad, Farrokh Aminifar, Amir Ghaedi , “Reliability modeling of run-of-the-river power plants in power system adequacy studies”, IEEE Transactions on Sustainable Energy, vol. 5, no. 4, pp. 1278-1286, 2014. DOI: 10.1109/TSTE.2014.2346462.

[4] Amir Ghaedi, Erfaneh Noroozi, “Reliability evaluation of renewable energy-based power system containing energy storage”, Advances in Science and Technology Research Journal, vol. 10, no. 32, pp. 198-205, 2016. DOI: https://doi.org/10.12913/22998624/65132.

[5] Mostafa Mirzadeh, Mohsen Simab, Amir Ghaedi, “Adequacy studies of power systems with barrage-type tidal power plants”, IET Renewable Power Generation, vol. 13, no. 14, pp. 2612-2622, 2019. DOI: 10.1049/iet-rpg.2018.5325.

[6] Mostafa Mirzadeh, Mohsen Simab, Amir Ghaedi, “Reliability evaluation of power systems containing tidal power plant”, Journal of Energy Management and Technology, vol. 4, no. 2, pp. 28-38, 2020. DOI:10.22109/JEMT.2020.176501.1167.

[7] Amir Ghaedi, Khodakhast Nasiriani, Mehdi Nafar, “Spinning Reserve Scheduling in a Power System Containing OTEC Power Plants”, International Journal of Industrial Electronics, Control and Optimization, vol. 3, no. 3, pp. 379-391, 2020. DOI: 10.22111/ieco.2020.32602.1231.

[8] Sebastian Pfaffel, Stefan Faulstich, and Kurt Rohrig, “Performance and reliability of wind turbines: A review”, Energies, vol. 10, no. 11, 104, 2017. DOI: 10.3390/en10111904.

[9] Li Chunlai, Zhao Yang, Teng Yun, Hui Qian, Zhang Tieyan , “Photovoltaic power station integrated information system modeling and reliability evaluation method research”, Intelligent Computation Technology and Automation (ICICTA), 2017 10th International Conference on. IEEE, 2017. DOI: 10.1109/ICICTA.2017.52.

[10] Hugo Mendonca, Sergio Martinez, “A resistance emulation approach to optimize the wave energy harvesting for a direct drive point absorber”, IEEE Transactions on Sustainable Energy, vol. 7, no. 1, pp. 3-11, 2016. DOI: 10.1109/TSTE.2015.2466097.

[11] Alireza Najafi, Shahab Rezaee, and Farschad Torabi , “Sensitivity analysis of a closed cycle ocean thermal energy conversion power plant”, Renewable Energy and Distributed Generation (ICREDG), 2012 Second Iranian Conference on. IEEE, 2012. DOI: 10.1109/ICREDG.2012.6190461.

[12] Yue Chen, Feng Liu, Wei Wei, Shengwei Mei, Naichao Chang, “Robust unit commitment for large-scale wind generation and run-off-river hydropower”, CSEE journal of power and energy systems, 2(4), 66-75, 2016. DOI: 10.17775/CSEEJPES.2016.00051.

[13] Pedro Bezerra Leite, Osvaldo R. Saavedra, Luiz Antonio de Souza Ribeiro, “Analysis of a tidal power plant in the estuary of Bacanga in Brazil taking into account the current conditions and constraints”, IEEE Transactions on Sustainable Energy, vol. 8, no. 3, pp. 1187-1194, 2017. DOI: 10.1109/TSTE.2017.2666719.

[14] Mingjun Liu, Wenyuan Li, Caisheng Wang, Roy Billinton, Juan Yu, “Reliability evaluation of a tidal power generation system considering tidal current speeds”, IEEE Transactions on Power Systems, vol. 31, no. 4, 3179-3188, 2015. DOI: 10.1109/TPWRS.2015.2473797.

[15] Roy Billinton, Ronald N. Allan, “Reliability Evaluation of Power Systems”, Plenum Press, New york and London, 2nd Edition, 1994.

[16] R.N. Allan, R. Billinton, N.M.K. Abdel-Gawad, “The IEEE reliability test system-extensions to and evaluation of the generating system”, IEEE Transactions on Power Systems, vol. 1, no. 4, pp. 1-7, 1986. DOI: 10.1109/TPWRS.1986.4335006.

[17] Roy Billinton, and Wenyuan Li, “Reliability Assessment of Electric Power System Using Monte Carlo”, Plenum Press, New York, 1994.

[18] Grigg, C.; Wong, P.; Albrecht, P.; Allan, R.; Bhavaraju, M., , “The IEEE Reliability Test System-1996. A report prepared by the Reliability Test System Task Force of the Application of Probability Methods Subcommittee”, IEEE Transactions on Power Systems, vol. 14, no. 3, pp. 1010 – 1020, 1999. DOI: 10.1109/59.780914